RSC Advances

ROYAL SOCIETY OF CHEMISTRY

www.rsc.org/advances

A multistage drug delivery system was design, which showed with MMP-2 sensitive size shrinkable and enhanced penetration propertiy.

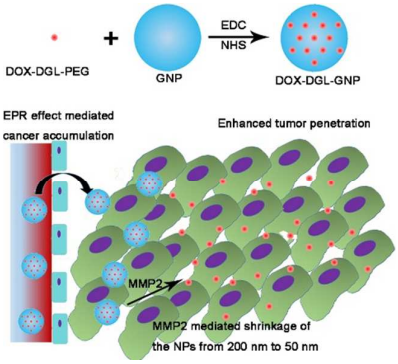

Multistage drug delivery system based on microenvironment-responsive dendrimer-gelatin nanoparticles for deep tumor penetration

Guanlian Hu[1], Yang Wang[1], Qin He[1]**, Huile Gao[1,2]*

[1]Key Laboratory of Drug Targeting and Drug Delivery Systems, West China School of Pharmacy, Sichuan University, No. 17, Block 3, Southern Renmin Road, Chengdu 610041, China;

[2]State Key Laboratory of Molecular Engineering of Polymers (Fudan University), Shanghai, 200433, China.

E-mail: gaohuile@scu.edu.cn (H. Gao), qinhe@scu.edu.cn (Q. He)

Abstract: A multistage drug delivery system was design, which showed with MMP-2 sensitive size shrinkable and enhanced penetration property.

Cancer is the second leading cause of death in the world and the high recurrence and mortality rate make it one of the greatest challenges in healthcare[1-3]. A successful nanoparticles (NP)-based strategy for the treatment of cancer is to not only effectively deliver drugs to cancer in order to improve the antitumor effect but also reduce drug-originated side effect[4]. A variety of NP have been commercially available, such as Doxil and Abraxane[5]. They accumulated to tumor tissues mainly relying on the enhanced permeability and retention (EPR) effect[6, 7]. However, because of the dense tumor extracellular matrix (ECM), abnormalities and shortage of the tumor vasculature and high interstitial fluid pressure (IFP), these NP of fixed size just passively accumulated around

the leaky tumor vasculature and couldn't be delivered throughout the entire tumor tissue with homogeneous drug concentration[8, 9]. All these microenvironments of tumor made the drugs cannot be effectively delivered to all cancer cells throughout the tumor[10, 11]. Therefore, constructing a drug delivery system which can not only retain in the tumor but also possess good penetration efficiency to the deep tumor tissue is of great importance to cancer treatment.

Particle size has a great effect on tumor penetration and retention of NP[12-16]. Generally, the smaller particle size is, the stronger tumor penetration ability of NP possess[17, 18]. In contrast, the tumor retention of NP was positively related with particle size, which meant NP with larger size (100~200 nm) had a significantly better tumor retention than smaller NP[12, 19, 20]. The requirements of tumor penetration and tumor retention for particle size were contradictory to each other, which the conventional drug delivery systems could not satisfy them successfully.

To reconcile this contradiction, multistage drug delivery systems were proposed with shrinkable size in response to specific stimuli in tumor[8, 21, 22], including in low pH[22-24] and high concentrations of matrix metalloproteinases (MMPs)[8], or external stimuli such as irradiation[11, 20]. Dendritic poly-L-lysine (DGL) is a kind of dendrimers with size as small as 5 nm[25]. Due to the small size of DGL, It may have strong penetrability into tumor tissues. Thus DGL was utilized as drug carrier in this study. In the meantime, gelatin is an animal-source compound that could be effectively hydrolyzed into small biomolecules by gelatinases, including MMP-2 and MMP-9[26, 27], which are highly expressed by almost all tumors and have been widely used as a stimuli to trigger the responsive NP[28, 29], thus in

this study gelatin NP (GNP) were used as degradable cores. Therefore, doxorubicin (DOX, used as model drug) decorated DGL were conjugated on the surface of GNP to construct a MMP-2 sensitive shrinkable system: DOX-DGL-GNP (Figure 1). The system, with relative large size, could effectively target and retain in tumor which benefited from EPR effect. When DOX-DGL-GNP reached the dense interstitial matrix by extravating from the leaky vessels in tumor after long circulation, MMP-2 hydrolyzed the gelatin core into small molecules and thereby released actively targeted dendrimers with small size, significantly increasing their diffusional ability in the interstitial matrix and penetrating into the core of tumor tissue.

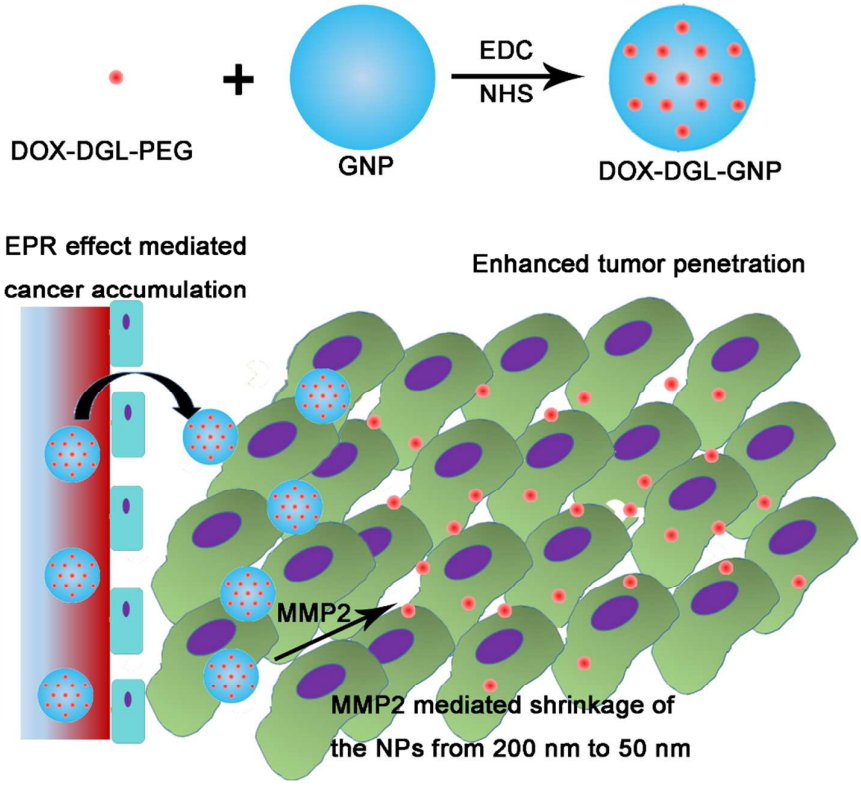

Figure 1. Schematic illustration to show the size shrinkage of the DOX-DGL- GNP from 200 nm to 50 nm triggered by MMP-2, a protease highly expressed in tumor extracellular matrix, thus penetrating into deep tumor tissue.

The diameter of DOX-DGL-PEG was approximately 30 nm (Table S1). After decorated onto GNP, the diameters of DOX-DGL-GNP was considerably increased to approximately 180 nm with a relatively narrow particle distribution. The increase of particle size indicated that small-sized DOX-DGL-PEG was successfully modified on the surface of GNP, which was consistent with our previous study[30].

In order to verify whether MMP-2 could degrade GNP or not, the particle sizes of DOX-DGL-GNP and DOX-DGL-PEG were recorded during the incubation with MMP-2 (460 ng/mL) at 37 ℃. Before incubation with MMP-2, the size of DOX-DGL-GNP was 177.0 ± 5.4 nm. During MMP-2 incubation expanding from 0 h to 24 h, the particle size was gradually decreased to 48.9 ± 1.4 nm (Figure 2A, B, C and D), suggesting the incubation with MMP-2 could effective make the DOX-DGL-GNP shrink from large size to small size. On the contrast, the size of DOX-DGL-PEG was stable (about 30 nm) during the incubation with MMP-2 (Figure 2A, B, E and F), indicating that the MMP-2 could not degrade the DGL. The result suggested the multistage nanocarrier DOX-DGL-GNP possessed MMP-2 sensitive shrinkable property.

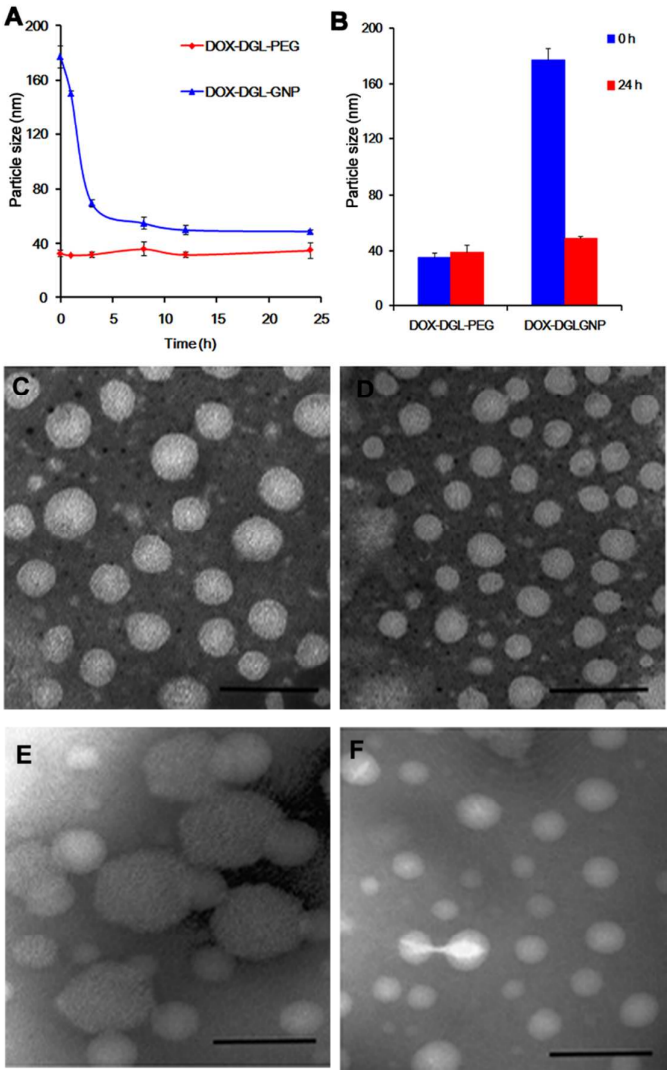

Figure 2. Size change of DOX-DGL-GNP in response to MMP-2. (A) The size change of DOX-DGL-PEG, DOX-DGL-GNP after MMP-2 digestion measured by dynamic light scattering. (B) The size of DOX-DGL-PEG, DOX-DGL-GNP at 0 h and 24 h during incubation with MMP-2. (C) TEM images of DOX-DGL-PEG before incubation with MMP-2. (D) TEM images of DOX-DGL-PEG after incubation with MMP-2 for 24 h. (E) TEM images of DOX-DGL-GNP before incubation with MMP-2. (F) TEM images of DOX-DGL-GNP after incubation with MMP-2 for 24 h. Bar represents 100 nm.

The multicellular tumor spheroids (MCTs) were used to investigate the penetration efficiency of this multistage DOX-DGL-GNP triggered by MMP-2 in a vivo-like tumor. DOX is a small compound that should have well penetration ability, but in vivo, most of free drug would be directly trapped in the cell near the vasculature, thus the free DOX could not penetrate into the area far from vasculature[31]. However, in vitro, the concentration was much higher than that of in vivo, and the drug directly contact with the MCT, which would show better penetration effect than NP[32]. Since the in vitro penetration of free drug could not reflect the in vivo condition, the free DOX was not used as control in this study. The released DOX-DGL-PEG conjugates from DOX-DGL-GNP were able to penetrate as deep as small-sized DOX-DGL-PEG conjugates (Figure 3C). DOX-DGL-PEG showed higher intensity in all slices of the MCTs while the intensity of DOX-GNP treated MCTs was much lower, suggesting smaller-sized particles possessed better penetrating efficiency[5]. By comparison, the fluorescence of DOX-DGL-GNP incubated with MMP-2 was located inside the MCTs while the fluorescence of DOX-DGL-GNP was limited at the periphery of MCTs, this phenomenon was significantly obvious at 100 μm from the surface towards the core. The results confirmed that this multistage nanocarrier DOX-DGL-GNP could benefit from degradation by MMP-2, which facilitated penetration in tumor by virtue of their small size.

The small-sized DOX-DGL-PEG could be released from the large-sized DOX-DGL-GNP when degraded by MMP-2, thus significantly decreased the diffusional hindrance in tumor dense matrix, and that is the reason why this multistage nanocarrier with shrinkable size

could deliver drug to the tumor' s poorly accessible regions. To verify this hypothesis, a collagen gel was used to simulate the dense interstitial matrix of tumor tissue in vitro[8, 21, 23]. Confocal microscope was used to gain insight into the infiltration activities of each sample into the collagen gel. The collagen gel penetration of large-sized DOX-DGL-GNP before or after incubation with MMP-2 was compared with small-sized DOX-DGL-PEG as control. DOX-DGL-GNP exhibited considerably negligible penetration before degradation (Figure 3A). In contrast, the DOX-DGL-GNP after degraded by MMP-2 was able to penetrate about 500 μm depth into the gel (Figure 3B). Besides, the released DOX-DGL-PEG exhibited similar infiltration activities as the free DOX-DGL-PEG (Figure 3B). The results demonstrated the penetration ability of this multistage DOX-DGL-GNP in collagen matrix significantly increased after cleavage by MMP-2, which was consistent with MCTs penetration study.

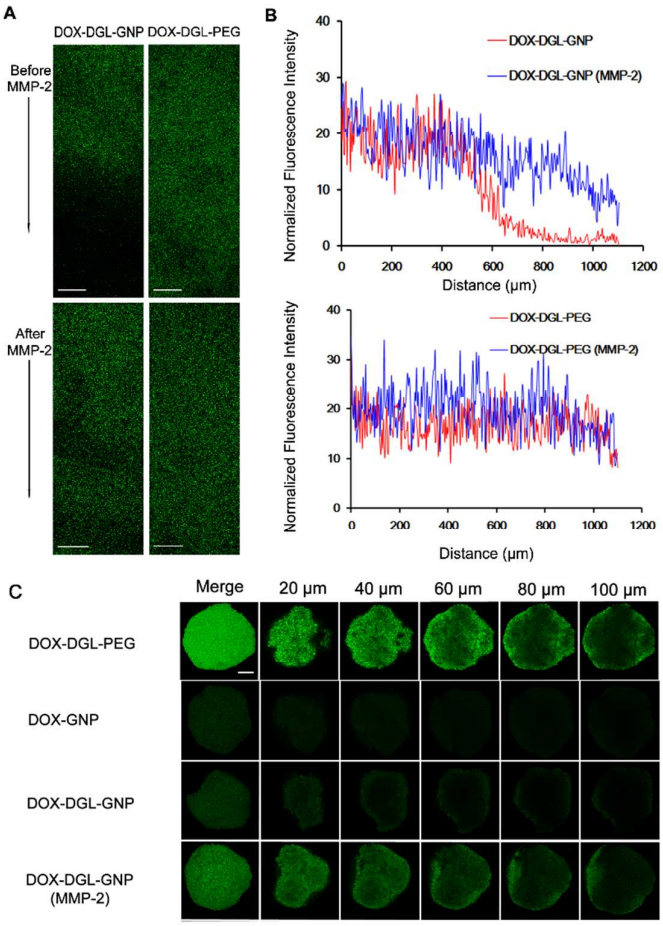

Figure 3. (A) Penetration profiles of DOX-DGL-GNP and DOX-DGL-PEG (before and after cleavage by MMP-2) in a collagen hydrogel mimicking the dense matrix of tumor tissue. Scale bars represent 125 μm. (B) Normalized fluorescent intensity profile of DOX-DGL-GNP and DOX-DGL-PEG after MMP-2 degradagation in collagen gel. (C) Fluorescent images of 4T1 MCTs after incubation with different formulations for 24 h. Scale bars represents 100 μm.

There are many studies have published that reported stimuli responsive NP, including drug release, size change, morphology alternation, etc.[28, 29]. Among of which, size shrinkable NP has gained much attention because their superiority in improving tumor penetration and retention. Previously, we had demonstrated gold NP fabricated onto GNP

could enhance the tumor targeting effect of gold NP[30, 33]. In this study, we further demonstrated polymeric NP, DGL, also could be effectively fabricated onto GNP, resulting a size-shrinkable system, which could be used as a good platform for drug delivery. However, this was only preliminary study, further evaluation, including the in vitro and in vivo distribution, toxicity and antitumor effect should be performed to fully evaluate the constructed NP.

In summary, a multistage nanocarrier, DOX-DGL-GNP, was constructed and evaluated. Based on the MMP-2 sensitive size shrink, the DOX-DGL-GNP delivered the DOX to the least accessible area of solid tumor, the core in tumor tissues. We believe that this study provide a facile strategy towards the design of more intelligent nanocarriers for deep tumor penetration in future.

Materials and methods

Synthesis of DOX-DGL-PEG conjugates. Detailed information about synthesis of DOX-DGL-PEG can be found in supporting information. Firstly, cis-aconityl doxorubicin (CAD) was synthesized by using mature reaction steps[34]. Secondly, DGL was reacted with NHS-PEG_{3400} at the ratio 1: 8 (molar ratio) in PBS (pH 8.0) for 2 h next the mixture was purified by ultrafiltration[35-37]. Next DGL-PEG was freeze-dried and analyzed in a 400 MHz spectrometer. At last, the carboxyl groups of CAD (42.0 mg, 60 μmol) were reacted with the amino groups of PEG–DGL in the presence of EDC (28.2 mg, 209 μmol) and NHS (12.4 mg, 106 μmol) in the dark for 4 hours[38], after addition of PEG–DGL in 3 mL of PBS (CAD : PEG–DGL= 48 : 1, molar ratio), the mixture was kept reaction in the dark for

12 h. Then the mixtures were purified by ultrafiltration through a membrane (MWCO10,000), and the amount of DOX conjugation was confirmed by UV-Vis spectrophotometry at 480 nm[34].

Preparation of GNP. GNP were prepared by a two-step desolvation method as previous described with some modification[8]. 12.5 mL of acetone was added to the gelatin type A (5% w/v, 12.5 mL) solution at 6.0 mL/min. After finishing addition exactly 1 min, the white colored supernatant was discarded and the gel-like precipitate was redissolved in deionized water (8 mL) at 40 °C. Next the pH value was adjusted to 2.7 with HCl (1 M)[39]. Under constant stirring at 600 rpm and 40 °C, acetone was slowly added at 1 mL/min until the solution appeared white milk-like, then glutaraldehyde solution (25%, 60 μL) in acetone (1 mL) was added at 0.05 mL/min. Subsequently, the solution was kept at 40 °C and 600 rpm for 7 h. At last, the acetone was removed by a rotary evaporator and the remaining solution was filtered through a 0.22 μm syringe filter. Glycine solution (1 M, 0.2 mL) was added and the GNP were stored overnight at 4 °C until used. A 1 mL solution of the GNP was injected into a Sephadex G-50 column (3.0 × 50 cm) eluted with PBS. The concentration of solid material in the suspension was usually as high as 20-25 mg/mL.

Preparation of DOX-DGL-GNP. EDC (0.8 mg, 4.2 μmol) and NHS (0.8 mg, 3.8 μmol) were added to the GNP solution (pH 6.0, 1 mL)[8]. After 30 min the pH value was adjusted to 8.0, a solution of COOH-PEG_{5000}-NH_2 (20 mg, ≈ 4 μmol) was added to the mixture. Next the reaction was carried out for 2 h and the pH was adjusted to 6.0, then an additional solution of EDC (0.8 mg) and sulfo-NHS (0.8 mg) dissolved in 50 μL of DI water was added. After stirring for 30 min, the pH value was adjusted to 8.0 again[8], DOX-DGL-PEG

(equivalent to 0.5 mg DOX, 1 mL) was added to the resulting mixture. The mixtures were purified by ultrafiltration through a membrane (MWCO 100,000) (4500 g × 30 min).

Degradation of GNP triggered by MMP-2 *in vitro*. The size change of DOX-DGL-PEG or DOX-DGL-GNP in response to MMP-2 was measured by a dynamic light scattering detector (Nano-ZS, Malvern, UK). DOX-DGL-PEG or DOX-DGL-GNP (0.2 mg) was incubated with 460 ng MMP-2 (50 mM Hepes, 2 mM $CaCl_2$) at 37 ℃ with gentle shaking for 24 h. The morphology of DOX-DGL-PEG or DOX-DGL-GNP was described via TEM.

Penetration assay using MCTs. The in vitro 4T1 MCTs were performed using the liquid overlay method. A certain amount of low melting point agarose was dissolved in RPMI 1640 (2%, m/v) and the solution was heated at 80 ℃ until completely dissolved. 100 μL of sterile agarose solution (2%, m/v) was added into each well of 96-well plates. Subsequently, 4T1 cells were seeded into each well at the density of 8×10^3 cells per well. The 96-well plates were gently shaken after seeding. The MCTs were allowed to grow up to a diameter about 300–400 μm for 2 days at 37 ℃ and 5% CO_2 in incubator. The uniform and compact MCTs were selected for the following studies. The MCTs were treated with different formulations at DOX concentration of 12.5 μg/mL for 24 h. Then, the MCTs were carefully washed thrice with cold PBS (pH 7.4), fixed with 4% paraformaldehyde for 30 min and placed in 96-well plates for confocal observation. The semi-quantitative analysis of the mean fluorescence intensity of DOX in MCTs was obtained by the software of confocal laser microscope.

Collagen Gel Diffusion. To further explore whether the tumor penetration of multistage nanocarrier after degradation increased or not, collagen hydrogels were used to simulate

the dense matrix of tumor tissue, which were prepared by mixing 141.75 μL rat tail collagen I (about 4 mg/mL), 3.8 μL sodium hydroxide (1 M) and 19.5 μL EDTA (0.17 M) on ice[8]. After vortexed for 5 min, the collagen hydrogels were added to partially fill a microslide capillary tube following by 12 h incubation at 37 °C. DOX-DGL-PEG or DOX-DGL-GNP (0.1 mg) were incubated with 230 ng of activated MMP-2 in 50 mM Hepes, 2 mM $CaCl_2$ for 24 h, respectively. At the end of 24 h, EDTA was added to adjust a final concentration to 20 mM. 20 μL of samples were carefully added into the capillary tube and the whole process of adding samples should ensure each sample was fully in contact with the surface of the gel. The sample was left at 37 ℃ for 12 h and then used for observing the distribution of fluorescence intensity of DOX via a confocal laser scanning microscopy at a wavelength of 560–590 nm.

Acknowledgements

This work was supported by the National Natural Science Foundation of China (81402866) and the National Basic Research Program of China (973 Program, 2013CB932504).

References

1. D. A. Corley, C. D. Jensen, A. R. Marks, W. K. Zhao, J. K. Lee, C. A. Doubeni, A. G. Zauber, J. de Boer, B. H. Fireman, J. E. Schottinger, V. P. Quinn, N. R. Ghai, T. R. Levin and C. P. Quesenberry, *N. Engl. J. Med.*, 2014, **370**, 1298-1306.
2. H. Z. Chen, S. Y. Tsai and G. Leone, *Nat. Rev. Cancer*, 2009, **9**, 785-797.

3. S. R. A. Wentong Lu, Dulal Senapati, Anant K. Singh, Tahir Arbneshi, Sadia Afrin Khan, and a. P. C. R. Hongtao Yu, *ACS Nano*, 2010, **4**, 10.

4. J. N. Benjamin Le Droumaguet, Davide Brambilla, Simona Mura, Andrei Maksimenko, E. S. Line De Kimpe, Cristiano Zona, Cristina Airoldi, Mara Canovi, Marco Gobbi, B. L. F. Magali Noiray, Francesco Nicotra, Wiep Scheper, Orfeu Flores, Massimo Masserini and a. P. C. Karine Andrieux, *ACS Nano*, 2012, **6**.

5. H. Cabral, Y. Matsumoto, K. Mizuno, Q. Chen, M. Murakami, M. Kimura, Y. Terada, M. R. Kano, K. Miyazono, M. Uesaka, N. Nishiyama and K. Kataoka, *Nat. nanotechnol.*, 2011, **6**, 815-823.

6. X. Guo, C. Shi, J. Wang, S. Di and S. Zhou, *Biomaterials*, 2013, **34**, 4544-4554.

7. X. Wang, X. Zhen, J. Wang, J. Zhang, W. Wu and X. Jiang, *Biomaterials*, 2013, **34**, 4667-4679.

8. C. Wonga, *P. N. A. S.*, 2011, **108**, 2427.

9. S. Park, S. Kang, X. Chen, E. J. Kim, J. Kim, N. Kim, J. Kim and M. M. Jin, *Biomaterials*, 2013, **34**, 598-605.

10. T. I. Minchinton AI, *Nat. Rev. Cancer*, 2006, **6**, 583–592.

11. R. Tong, H.H. Chiang and D.S. Kohane, *P. N. A. S.*, 2013, **110**, 19048-19053.

12. C. He, Y. Hu, L. Yin, C. Tang and C. Yin, *Biomaterials*, 2010, **31**, 3657-3666.

13. B. Devika Chithrani, Arezou A. Ghazani, and Warren C. W. Chan, *Nano Lett.*, 2006, **6**, 662-668.

14. D. Ding, J. Wang, Z. Zhu, R. Li, W. Wu, B. Liu and X. Jiang, *ACS Appl. Mater. Inter.*, 2012, **4**, 1838-1846.

15. E. Vlashi, *ACS Nano*, 2013, **7**, 8573-8582.

16. L. Tang, N. P. Gabrielson, F. M. Uckun, T. M. Fan and J. Cheng, *Mol. Pharm.*, 2013, **10**, 883-892.

17. N. D. He Dong, Jessica Y. Shu, JaiW. Seo, Lisa M. Mahakian, KatherineW. Ferrara,and and T. Xu, *ACS Nano*, 2012, **6**.

18. S. Huo, H. Ma, K. Huang, J. Liu, T. Wei, S. Jin, J. Zhang, S. He and X. J. Liang, *Cancer Res.*, 2013, **73**, 319-330.

19. Steven D. Perrault, *Nano Lett.*, 2009, **9**, 1909-1915.

20. R. Tong, H. D. Hemmati, R. Langer and D. S. Kohane, *J. Am. Chem. Soc.*, 2012, **134**, 8848-8855.

21. J. Li, Y. Han, Q. Chen, H. Shi, S. ur Rehman, M. Siddiq, Z. Ge and S. Liu, *J. Mater. Chem. B*, 2014, **2**, 1813.

22. Y. Yu, X. Zhang and L. Qiu, *Biomaterials*, 2014, **35**, 3467-3479.

23. M. Zan, J. Li, S. Luo and Z. Ge, *Chem. Commun.*, 2014, **50**, 7824-7827.

24. Z. Cheng, Y. Dai, X. Kang, C. Li, S. Huang, H. Lian, Z. Hou, P. Ma and J. Lin, *Biomaterials*, 2014, DOI: 10.1016/j.biomaterials.2014.04.029.

25. N. Yevlampieva, A. Dobrodumov, O. Nazarova, O. Okatova and H. Cottet, *Polymers*, 2012, **4**, 20-31.

26. J. H. Xu, F. P. Gao, X. F. Liu, Q. Zeng, S. S. Guo, Z. Y. Tang, X. Z. Zhao and H. Wang, *Chem. commun.*, 2013, **49**, 4462-4464.

27. T.G. Shutava, S.S. Balkundi, D.P. O'Neal, Y.M. Lvov, P. Vangala, J. Steffan and R.L. Bigelow. ACS Nano, 2009, **3**, 1887-1885.

28. M. R. Dzamukova, E. A. Naumenko, Y. M. Lvov and R. F. Fakhrullin, *Sci. Rep.*, 2015, **5**, 10560.

29. A. P. Blum, J. K. Kammeyer, A. M. Rush, C. E. Callmann, M. E. Hahn and N. C. Gianneschi, *J. Am. Chem. Soc.*, 2015, **137**, 2140-2154.

30. S. Ruan, X. Cao, X. Cun, G. Hu, Y. Zhou, Y. Zhang, L. Lu, Q. He and H. Gao, *Biomaterials*, 2015, **60**, 100-110.

31. A. J. Primeau, A. Rendon, D. Hedley, L. Lilge and I. F. Tannock, *Clin. Cancer Res.*, 2005, **11**, 8782-8788.

32. T. Zong, L. Mei, H. Gao, W. Cai, P. Zhu, K. Shi, J. Chen, Y. Wang, F. Gao and Q. He, *Mol. Pharm.*, 2014, **11**, 2346-2357.

33. S. Ruan, Q. He and H. Gao, *Nanoscale*, 2015, **7**, 9487-9496.

34. C. Du, D. Deng, L. Shan, S. Wan, J. Cao, J. Tian, S. Achilefu and Y. Gu, *Biomaterials*, 2013, **34**, 3087-3097.

35. Y. Liu, J. Li, K. Shao, R. Huang, L. Ye, J. Lou and C. Jiang, *Biomaterials*, 2010, **31**, 5246-5257.

36. S. An, Y. Kuang, T. Shen, J. Li, H. Ma, Y. Guo, X. He and C. Jiang, *Biomaterials*, 2013, **34**, 8949-8959.

37. S. Huang, K. Shao, Y. Kuang, Y. Liu, J. Li, S. An, Y. Guo, H. Ma, X. He and C. Jiang, *Biomaterials*, 2013, **34**, 5294-5302.

38. S. Zhu, M. Hong, G. Tang, L. Qian, J. Lin, Y. Jiang and Y. Pei, *Biomaterials*, 2010, **31**, 1360-1371.

39. J. A. C. Tatsiana G. Shutava, Shantanu S. Balkundi, D. Patrick O'Neal,Yuri M. Lvov,Pranitha Vangala,Joshua J. Steffan,Rebecca L. Bigelow,, *ACS Nano*, 2009, **3**, 1887-1885.